Activated Carbon Prepared from *Alternanthera philoxeroides* Biomass by One-step K_2CO_3 Activation

Xian-fa Li,* Wen-ting Chen, and Lin-qin Dou

Activated carbons (ACs) were prepared from *Alternanthera philoxeroides* (AP) by K_2CO_3 one-step mixing activation. The effects of the mixing mass ratio of K_2CO_3 to AP, activation temperature, N_2 flow rate, and period on the yield and specific surface area of ACs were investigated. The results showed that the surface area and pore volume of ACs were closely related to activation conditions and that the activation temperature was the main factor influencing the surface area and pore volume. The activation conditions only had a slight effect on the yield of ACs, which varied between 13.5% and 19.5%. The surface area of 1799.8 m^2/g was obtained at a K_2CO_3 to AP mass ratio of 2:1, activation temperature of 900 °C, activation time of 2 h, and N_2 flow rate of 60 cm^3/min. The surface morphology of ACs were characterized with scanning electron microscopy (SEM), and the recovered K_2CO_3 was characterized with powder X-ray diffractometry (XRD). The SEM images of the ACs also showed that the activation temperature had an obvious effect on the porous structure.

Keywords: Activated carbon; Chemical activation; Potassium carbonate; Biomass waste; Alternanthera philoxeroides

Contact information: School of Life Science and Engineering, Southwest University of Science and Technology, Mianyang 621010, China;
** Corresponding authors: xfli816@ustc.edu.cn; lixianfa@swust.edu.cn*

INTRODUCTION

Alligator weed, *Alternanthera philoxeroides* (AP), is a prominent and problematic weed all over the world (Lu *et al.* 2010). AP is found on the upper surface of lakes, ponds, and wetlands. It grows rapidly in a short period of time and generally forms a dense, tangled mat (Schooler *et al*. 2007). Due to its prevalence, it shades the aquatic vegetation from sunlight and reduces water flow (Buckingham 1996). Alligator weed can also cause the death of fish and native plants and provides a favorable habitat for mosquitoes (Bhattacherjee *et al*. 2014). The control and elimination of AP includes biological (Sun *et al*. 2010; Wei *et al*. 2015), chemical, and physical methods (Schooler *et al*. 2008). Biological control is a valuable and environmentally friendly method of weed control. However, the efficiency of biological control is low, and only 33% of released agents successfully control target weeds (McFadyen 1998). There are also issues of ecological safety, and these agents can be dangerous to animals, including mammals (Cordeau *et al*. 2016). Compared with other methods, the chemical method is efficient in a short time (Willingham *et al.* 2015). However, it may cause environmental contamination and decrease biological diversity (Wei *et al.* 2010). Moreover, the limited serviceable range of chemical substances cannot remove the belowground roots, which may lead to the continued spreading of AP. The physical method, mechanical weeding, is useful for AP that has not formed a major infestation. However, the mowed rootstock needs to be disposed immediately; otherwise, AP will spread further. The main methods of physical

control are manual removal and disposal, but this approach creates secondary environmental problems, such as the release of pathogens and methane (Yang *et al*. 2014). Moreover, *in situ* stubble burning of AP is now banned because of the smoke and other hazards (Abouziena and Haggag 2016). However, the mowed rootstock being collected and used to produce ACs by a controlled high temperature catalytic pyrolysis can avoid spreading of AP and secondary environmental problems.

Activated carbon (AC) is the most popularly used adsorbent for removal of organic and metal ion pollutants (Hassan *et al*. 2013). AC obtained from biomass such as AP has the obvious advantages, such as environmental friendliness, efficiency, and low cost compared with non-renewable, coal-based activated carbons (Kucherenko *et al*. 2010; Yan and Sorial 2011). K_2CO_3 as an activating agent has low corrosion to facilities, less environmental damage than KOH and H_2SO_4 (Guo and Lua 1999), and extensive applications in AC production (Gurten *et al*. 2012). AP can be used for preparing AC by high temperature activation, which prevents the further spread of mowed AP. At present, very few studies have examined AC prepared form AP.

In this work, ACs were prepared from AP by K_2CO_3 one-step mixing activation. The effects of various process parameters, such as the mixing mass ratio of K_2CO_3 to AP, activation temperatures, N_2 flow rate and activation period, BET specific surface area, and the AC yield were investigated. The surface morphology of AC was characterized by scanning electron microscopy (SEM). The activation agent was recovered by rotary vacuum distillation and crystallization, and the recovered K_2CO_3 was characterized with powder X-ray diffractometry (XRD).

EXPERIMENTAL

Materials and Reagents

AP was collected from the garden in Southwest University of Science and Technology, Sichuan, China. The AP was cleaned, dried at 80 °C for 24 h, powdered, and screened by the 75 µm sieve to achieve uniform particle size. The sieved material was stored in a dryer until further use. Analytical-grade K_2CO_3 was purchased from the Sinopharm Chemical Reagent Co. (Chengdu, China). High-purity N_2 was obtained from the Mianyang Special Gases Factory (Minyang, China).

Preparation of the ACs

The preparation method of ACs from AP by K_2CO_3 activation was based on previous literature (Li *et al*. 2016). A total of 5 g of AP was physically mixed with powdery K_2CO_3 in a mass ratio range from 1:1 to 1:2. The mixed sample was set on a ceramic boat, which was inserted into a stainless steel reactor. The reactor was placed in a tube furnace (LENTON, Sheffield, UK) and heated at constant rate of 10 °C/min and held at different carbonization temperatures (500 to 900 °C) for different carbonization times (1 to 4 h) under different nitrogen flow rates (20 to 100 cm^3/min). The sample was cooled to room temperature in the furnace after activation under the same N_2 flow rate. The mixture was washed and filtered three times with 50 mL of circulating water. The filtrate was used to recover the activating agent by rotary evaporation and crystallization. The precipitate was thoroughly washed with hot distilled water to remove chemicals from the final products until the pH of the residual solution reached 6 to 7, and part of the washing water was reused for the next wash. The washed sample was oven-dried at 105 °C for 12 h and then

grinded to use for characterization.

ACs Characterization

The C, H, N, and O contents of AP and produced ACs were determined using a Vario ELIII (Langenselbold, Germany) instrument. The proximate analyses were developed according to ISO standards for moisture at 100 °C in air, ISO 589 (2008), volatile matter at 900 °C in N_2 atmosphere, ISO 562 (1974), and ash incineration at 815 °C in air, ISO 1171 (1976). The specific surface area, the pore volume, and the average pore diameter of ACs were determined using a N_2 adsorption automated analyzer (TriStar II 3020 V1.03, Micromeritics, Norcross, MA, U.S.A) at -196 °C to obtain the calculations from adsorption-desorption test data. The samples were degassed for 5 h to remove moisture and impure components on the surface in the vacuum environment at 300 °C before testing. The specific surface areas of AC were determined using the Brunauer-Emmett-Teller (BET) method (Brunauer *et al*. 1938). The total pore volumes (V_t) were calculated using the single adsorption assay of N_2 adsorption isotherm relative pressure of 0.973. The microporous volumes (V_{micro}) and external surface area (A_e) of AC were measured by the *t*-method. The average pore diameter of AC was calculated from N_2 adsorption isotherm by the Barrett-Joyner-Halenda (BJH) method (Barrett *et al*. 1951).

The yield of AC was calculated according to formula as follows,

$$Yield(\%) = \frac{Final\ mass\ of\ activated\ AP(\mathrm{g})}{Initial\ mass\ of\ AP(\mathrm{g})} \times 100\% \quad (1)$$

The surface morphology of AC was obtained by the EVO 18 tungsten filament scanning electron microscope (Zeiss, Oberkochen, Germany). Before observations, the surface of samples was sprayed with gold. The recovered K_2CO_3 activating agent was calculated according to the Eq. 2,

$$\text{Recovery ratio of } K_2CO_3(\%) = \frac{Mass\ of\ activated mixtures - Final\ mass\ of\ activated\ AP(\mathrm{g})}{Initial\ mass\ of\ K_2CO_3\ in\ activation(\mathrm{g})} \times 100\% \quad (2)$$

The recovered K_2CO_3 and analytical-grade K_2CO_3 were examined by an X-ray diffractometer (Philips X' Pert PRO SUPER, 2 kW, Almelo, The Netherlands) using Cu-Kα radiation with a scan speed of 2°/min.

Fourier-transform infrared (FT-IR) spectra were recorded in transmission mode using a Spectrum One 55 spectrometer (PerkinElmer Inc., Waltham, Massachusetts, U.S.A).

The composition and content of the ash in ACs were determined by X-ray fluorescence spectrometry (Axios, PANalytical, The Netherlands).

RESULTS AND DISCUSSION

The proximate and ultimate component analyses of the AP are shown in Table 1. The carbon content of AP was 40.32%, which was slightly lower than oxygen, and it had a high ash content of 10.56%. Moreover, the AP had high volatile matter (79.20%) and low fixed carbon content (5.64%), which was the main reason for the lower yield of AC than from of other materials, such as palm shell (Adinata *et al*. 2007).

The proximate and ultimate component analyses of the produced ACs are also

shown in Table 1. The content of fixed carbon decreased with the increase in the K_2CO_3 to AP mass ratio and the increased activation temperature. At the same time, the ash content increased with increasing of activation temperature and the mass ratio of K_2CO_3 to AP. The reason is most probably the increased burn-off of organic matter with increasing activation temperature and activating agent dosage. The content of K^+ of ACs at various activation conditions is in the range between 0.18 and 0.32% calculated from the data of ash content and X-ray fluorescence spectrometry (Axios, PANalytical, The Netherlands) by normalization method. The elemental analysis results of the produced ACs showed that the carbon content at various activation conditions no marked differences.

Table 1. Proximate and Ultimate Analyses of AP and Produced ACs

Materials	Proximate Analysis (wt.%) [a]				Ultimate Analysis (wt.%, dry basis)			
	Moisture	Fixed carbon	Volatile matter	Ash	C	H	N	O[b]
AP	4.58	5.66	79.20	10.56	40.32	5.63	0.99	52.72
$AC_{1\text{-}800\text{-}2\text{-}60}$	3.14	43.03	33.88	19.96	67.46	0.94	0.75	30.85
$AC_{1.5\text{-}800\text{-}2\text{-}60}$	3.11	36.83	35.17	24.89	66.37	0.74	0.77	32.12
$AC_{2\text{-}800\text{-}2\text{-}60}$	5.38	24.81	38.24	31.57	64.91	1.02	0.93	33.14
$AC_{2\text{-}800\text{-}2\text{-}20}$	2.66	46.25	29.01	22.08	66.44	0.69	0.86	32.01
$AC_{2\text{-}800\text{-}3\text{-}60}$	2.88	41.28	34.88	20.96	66.34	0.72	0.76	32.18
$AC_{2\text{-}700\text{-}2\text{-}60}$	6.76	35.70	39.87	17.68	63.11	1.58	1.48	33.83
$AC_{2\text{-}900\text{-}2\text{-}60}$	5.40	19.71	40.09	34.79	66.61	1.07	0.80	31.52
a: dry basis, b: by difference								
Nomenclature = $AC_{R\text{-}T\text{-}t\text{-}v}$; where R is K_2CO_3 to AP mass ratio, T is activation temperature (°C), t is dwell time (h), and v is N_2 flow rate (cm^3 / min)								

The effect of the mass ratio of K_2CO_3 to AP on the yield, surface area, and pore volumes of AC are shown in Table 2 (entries 1 to 3). The mass ratio had an influence on the AC yield. When the mass ratio increased from 1 to 2, the AC yield increased from 14.2% to 17.1%. The probable reason for AC yield increase was due to the dehydration action. The main components of AP were saccharides with a little of lignin. With the increased of K_2CO_3, the hexose and pentose were dehydrated rapidly, and they formulated a polyaromatic ring structure, which can inhibit the escape of volatile.

Table 2. Textural Characteristics of ACs Obtained from AP by K_2CO_3 Activation

Entry	$AC_{R\text{-}T\text{-}t\text{-}v}$	A_{BET} (m^2/g)	A_e (m^2/g)	V_t (cm^3/ g)	V_{micro} (cm^3/ g)	V_{micro}/V_t (%)	D (nm)	Y (%)
1	$AC_{1\text{-}800\text{-}2\text{-}60}$	1118.7	231.4	0.568	0.415	73.1	2.0	14.2
2	$AC_{1.5\text{-}800\text{-}2\text{-}60}$	1163.4	191.2	0.556	0.453	80.9	1.9	15.8
3	$AC_{2\text{-}800\text{-}2\text{-}60}$	1191.6	176.5	0.569	0.472	83.0	1.9	17.1
4	$AC_{2\text{-}800\text{-}2\text{-}20}$	1302.6	270.4	0.628	0.474	75.5	1.9	16.5
5	$AC_{2\text{-}800\text{-}2\text{-}100}$	1185.5	206.2	0.583	0.455	78.0	2.0	18.3
6	$AC_{2\text{-}800\text{-}1\text{-}60}$	1163.6	149.2	0.569	0.470	82.6	2.0	17.5
7	$AC_{2\text{-}800\text{-}3\text{-}60}$	1455.6	410.2	0.717	0.487	67.9	2.0	13.8
8	$AC_{2\text{-}800\text{-}4\text{-}60}$	1341.2	248.5	0.645	0.507	78.6	1.9	13.5
9	$AC_{2\text{-}700\text{-}2\text{-}60}$	771.3	102.9	0.384	0.312	81.2	2.0	19.5
10	$AC_{2\text{-}900\text{-}2\text{-}60}$	1799.8	1095.6	0.926	0.314	33.9	2.1	15.6
Nomenclature = R-T-t-v; where R is K_2CO_3 to AP mass ratio, T is activation temperature (°C), t is dwell time (h), and v is N_2 flow rate (cm^3 / min)								

The effect of the mass ratio of K_2CO_3 to AP on the surface area of AC and the pore volume was not obvious. When the mass ratio of K_2CO_3 to AP was increased from 1 to 2, the BET surface area of AC only increased from 1118.7 to 1191.6 m^2/g. The total pore volumes were almost unchanged, while the micropore volumes slightly increased from 0.415 to 0.472 cm^3/g. In addition, under different K_2CO_3 to AP mass ratios, ACs were mainly microporous structures. Based on the results of yield and surface area, the mixing mass ratio of K_2CO_3 to AP of 2:1 was used in subsequent experiments.

The effect of N_2 flow rate on the AC yield is shown in Table 2 (entries 3 to 5). An increasing N_2 flow rate led to a slight increase in the AC yield. This result suggests that with the increasing N_2 flow rate, the auxiliary activating agent CO, CO_2, and steam, which were generated during the activation, were flushed away rapidly. Thus, the activation level decreased, and the carbon yield increased. The effect of N_2 flow on the BET surface area and the AC pore volume is shown in the 3rd to 5th rows of Table 2. With the N_2 flow increasing from 20 mL/min to 100 mL/min, the BET surface area of AC was reduced from 1302.6 m^2/g to 1185.5 m^2/g. Increasing the N_2 flow rate resulted in the rapid disappearance of CO, CO_2, and steam generated during activation. Hence, increasing the N_2 flow rate slightly decreased the surface areas and pore volumes.

The effects of activation time on the AC yield are shown in Table 2 (entry 3 and entries 6 to 8). With the extension of the activation time, there was a slight decrease in the AC yield because of oxidative aging of carbon with CO_2 or steam produced from volatiles. When the activation time was 1 h, the BET surface area and total pore volume of AC were 1163.6 m^2/g and 0.569 cm^3/g, respectively. When the time was prolonged to 3 h, the BET surface area and the total pore volume of AC increased to 1455.6 m^2/g and 0.717 cm^3/g, respectively. At an activation time to 4 h, there was a slight decrease in the BET surface area and total pore volume. Thus, the best activation time for AC prepared from AP by K_2CO_3 one-step mixing activation was 3 h.

The effect of activation temperature on the AC yield is shown in Table 2 (entry 3 and entries 9 to 10). When the temperature was 700 °C, the AC yield was 19.5%. When the activation temperature increased to 900 °C, the AC yield was only 15.6%. Hence, increasing the activation temperature resulted in the degree of activation increasing, so the AC yield was decreased.

The effect of activation temperature on the surface area and the pore volume are shown in Table 2 (entry 3 and entries 9 to 10). When the activation temperature was 700 °C, the BET surface area and total pore volume was only 771.3 m^2/g and 0.384 cm^3/g, respectively. When the activation temperature was raised to 900 °C, the BET surface areas and pore volume increased to 1799.8 m^2/g and 0.926 cm^3/g, respectively; the ratio of micropore volume was decreased from 81.2% to 33.9%. Moreover, with increasing activation temperature, the degree of activation increased, and the AC surface area increased. This resulted in part of microporous carbons being expanded further at the higher temperature, growing, and forming mesoporous carbons. Thus, the microporous area decreased as the mesoporous volume increased.

Figure 1 shows the N_2 adsorption-desorption isotherms of ACs prepared at different activation temperatures. With increasing activation temperature, the N_2 adsorption capacity of AC increased. When the activation temperatures were between 700 and 800 °C, the adsorption curve was a typical adsorption isotherm of type I, which was characterized with micropore structures. When the activation temperature was increased to 900 °C, the adsorption-desorption isotherms of AC exhibited an apparent hysteresis loop, which is evidence of the presence of mesopores.

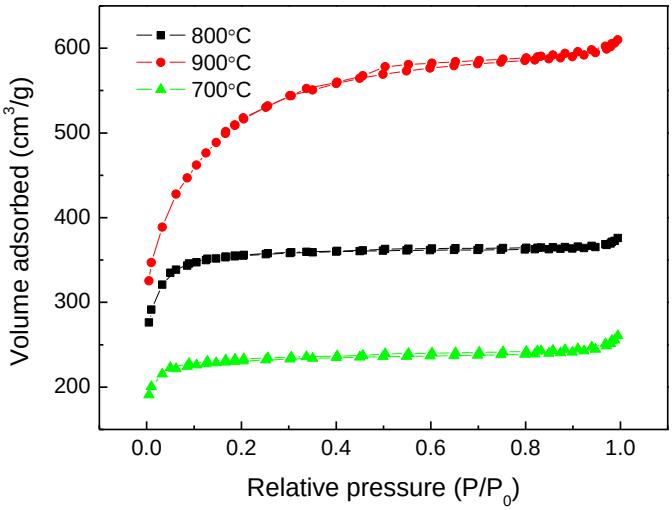

Fig. 1. Nitrogen adsorption/desorption isotherms of AC obtained by K_2CO_3 at various activation temperatures

SEM images of the ACs activated at various temperature are shown in Fig. 2.

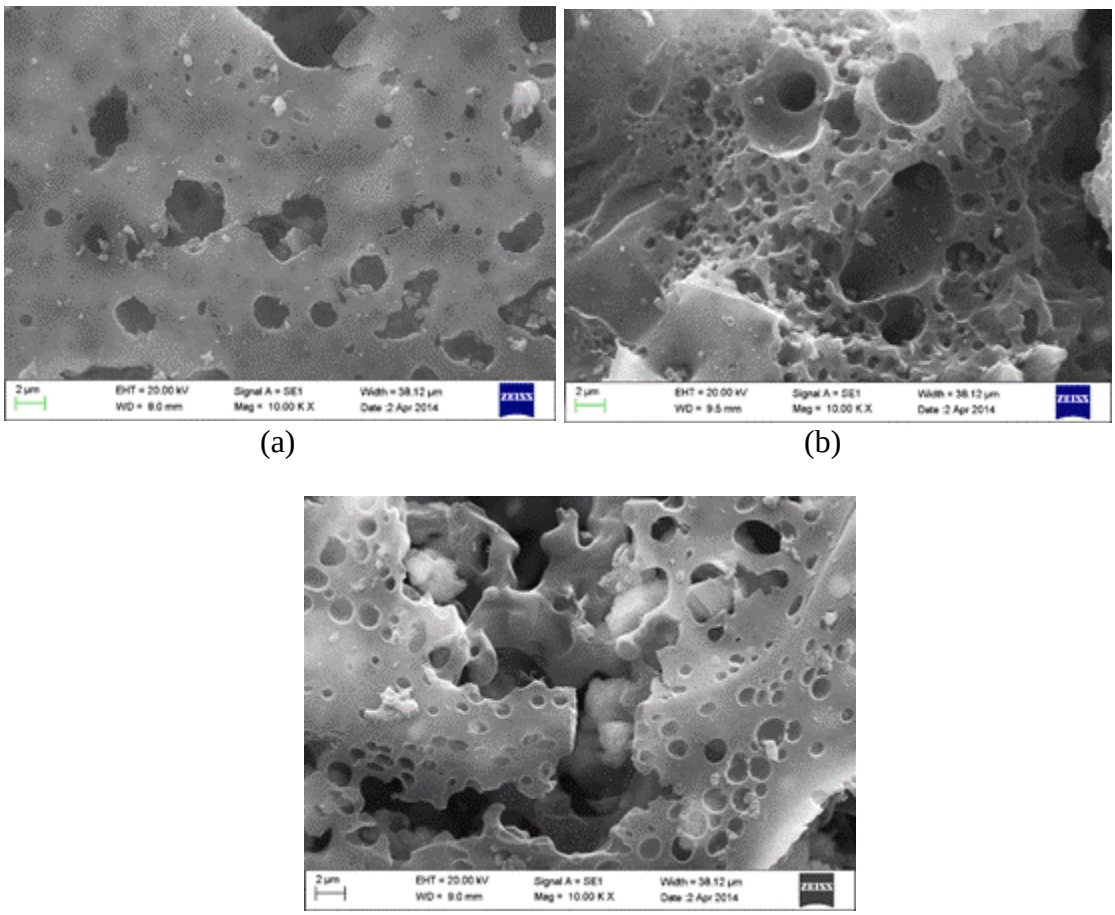

(a) (b)

(c)

Fig. 2. SEM images of ACs prepared at (a) 700 °C, (b) 800 °C, and (c) 900 °C (mass ratio: 2.0，activation time: 2 h，N_2 flow rate: 60 mL/min)

With increasing temperature, a gradual change in AC surface morphology was observed. For the AC activated at 700 °C, the surface was smoother and less porous than in the samples activated at 800 °C and 900 °C. The AC obtained at 900 °C had comparatively good homogeneous porous surface morphology, which indicated a higher BET surface area than that of 700 °C and 800 °C. Moreover, at 900 °C, more macropores and cavities were observed due to micropore enlarging to mesopores and macropores, which was consistent with the decreased micropore volume of AC (33.9%).

The Fourier transform infrared (FT-IR) spectra of the ACs obtained at various activation temperature are shown in Fig. 3. As shown in the figure, the ACs had similar chemical composition with rare surface functional groups, indicating that the produced ACs have stable chemical property with a low content of oxygen-containing functional groups.

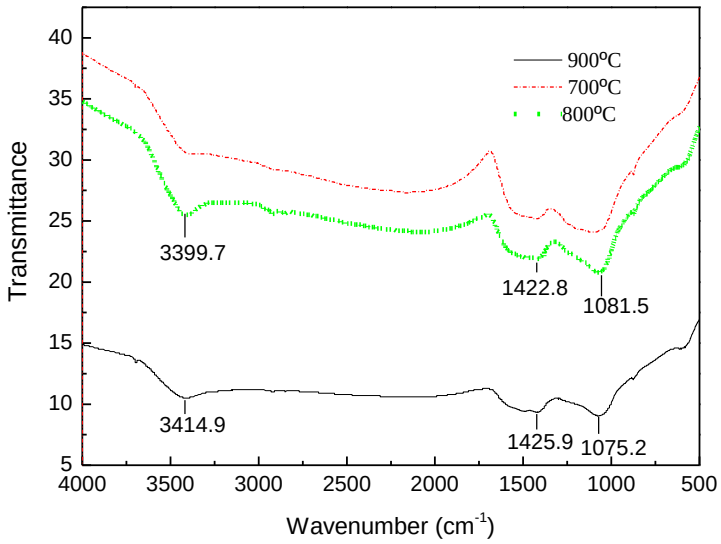

Fig. 3. FT-IR spectra of the ACs obtained at various activation temperature

The recovery ratios of K_2CO_3 used at 500 to 900 °C are shown in Fig.4. As shown, when the activation temperature was lower than 800 °C, the reduced range of the recovery ratio of K_2CO_3 was not significant. When the activation temperature exceeded 800 °C, the recovery ratio of K_2CO_3 was significantly reduced. A possible reason was that K_2CO_3 melts at high temperature (891 °C), becomes oxidized by carbon to CO, and forms the element K in vapor. The element K, which has a lower boiling point (774 °C), was taken out of the activation furnace by the N_2 flow, so the recovery rate was greatly reduced. This trend was consistent with previous results reported by Hayashi *et al*. (2000).

The reaction mechanism was as follows: $K_2CO_3 + 2C \rightarrow 2K + 3CO$.

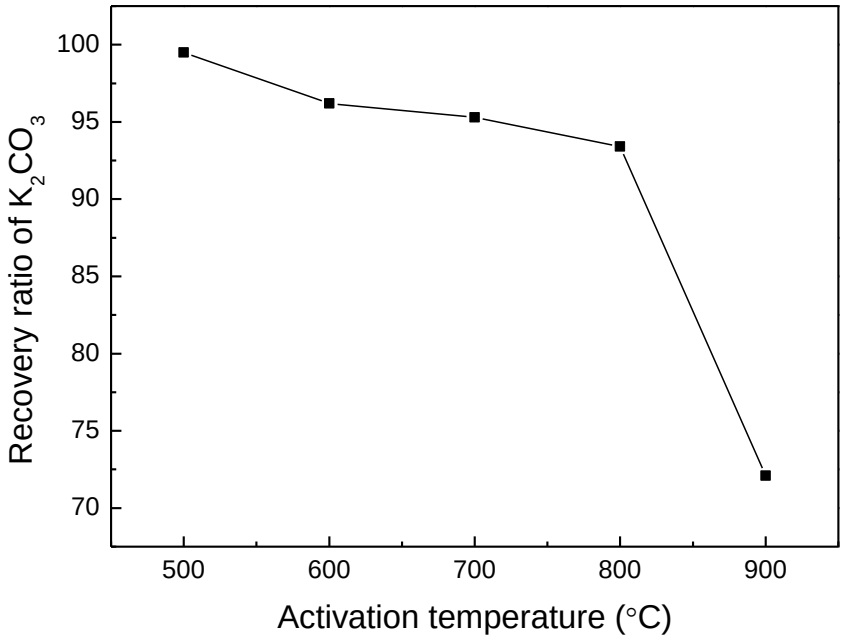

Fig. 4. Recovery ratio of K_2CO_3 at various activation temperatures (mass ratio: 2.0, activation time: 2 h，N_2 flow rate: 60 mL/min)

The XRD patterns of recovered K_2CO_3 and chemical reagents K_2CO_3 were measured. As shown in Fig. 5, the characteristic peak of recovered K_2CO_3 and chemical reagents of K_2CO_3 were similar. The recovered K_2CO_3 mainly existed in two forms: $K_2CO_3 \cdot 1.5H_2O$ and K_2CO_3. K_2CO_3 has strong water absorption, which accounts for the peaks of $K_2CO_3 \cdot 1.5H_2O$. This result showed that the major component of recovered activating agent was K_2CO_3. The original K_2CO_3 was main $K_2CO_3 \cdot 1.5H_2O$, as determined by searching XRD standard spectrum index. The original K_2CO_3 and recovered K_2CO_3 appear to be an obvious decaying pattern, which may be due to the existing amorphous composition.

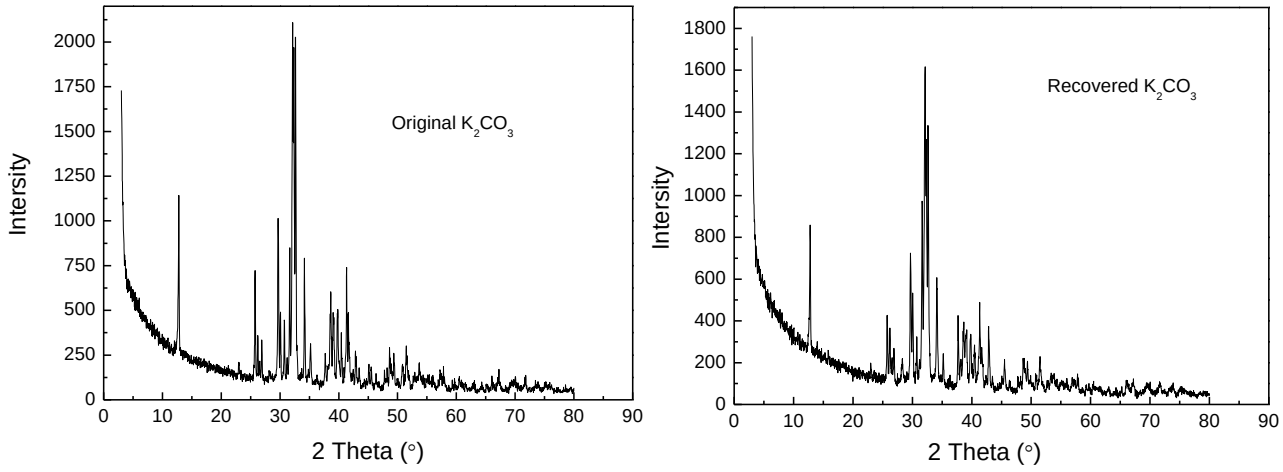

Fig. 5. XRD images of recovered K_2CO_3 and original K_2CO_3

CONCLUSIONS

1. To control the spread of the invasive plant *Alternanthera philoxeroides* (AP) and efficiently utilize AP, activated carbons (ACs) were prepared from AP by K_2CO_3 one-step mixing activation to obtain the high specific surface areas and the pore volumes of AC. The activating agent, K_2CO_3, can be recovered partially, and the amount of washing water and the discharge of wastewater can be reduced.
2. When the mass ratio of K_2CO_3 to AP was 2:1, the activation temperature was 900 °C, the activation time was 2 h, and the N_2 flow rate was 60 cm^3/min; the surface area of AC reached 1799.8 m^2/g.
3. The SEM result of AC showed that activation temperature had an obvious effect on the pore structures and morphology. The XRD result showed that the main recovered component was still K_2CO_3.

ACKNOWLEDGMENTS

This work was supported by Key Project of Education Department of Sichuan province (14ZA0092), Doctor Foundation (14zx7155) of Southwest University of Science and Technology in China, Innovation Team building fund project of Sichuan Provincial Biomass Modified Materials Engineering Research Center in China (14tdgc02), and Sichuan Science Foundation (2015JY0015).

REFERENCES CITED

Abouziena, H. F., and Haggag, W. M. (2016). "Weed control in clean agriculture: A review," *Planta Daninha* 34(2), 377-392. DOI: 10.1590/S0100-83582016340200019

Adinata, D., Daud, W. M. A., and Aroua M. K. (2007). "Preparation and characterization of activated carbon from palm shell by chemical activation with K_2CO_3," *Bioresource Technology* 98(1), 145-149. DOI: 10.1016/j.biortech.2005.11.006

Barrett, E. P., Joyner, L. G., Halenda, P. P. (1951). "The determination of pore volume and area distributions in porous substances. I. Computations from nitrogen isotherms," *Journal of the American Chemical Society* 73, 373-380. DOI: 10.1021/ja01145a126

Bhattacherjee, A., Ghosh, T., Sil, R., and Datta. A. (2014). "Isolation and characterisation of methanol-soluble fraction of *Alternanthera philoxeroides* (Mart.) – Evaluation of their antioxidant, α-glucosidase inhibitory and antimicrobial activity in *in vitro* systems," *Natural Product Research* 28(23), 2199-2202. DOI: 10.1080/14786419.2014.930857

Brunauer, S., Emmett, P. H., and Teller, E., (1938). "Adsorption of gases in multimolecular layers," *Journal of the American Chemical Society* 60, 309-319. DOI: 10.1021/ja01269a023

Buckingham, G. R. (1996). "Biological control of alligator weed, *Alternanthera philoxeroides*, the world's first aquatic weed success story," *Castanea* 61(3), 232-243. Stable URL: http://www.jstor.org/stable/4033676

Cordeau, S., Triolet, M., Wayman, S., Steinberg, C., and Guillemin J. P. (2016). "Bioherbicides: Dead in the water? A review of the existing products for integrated weed management," *Crop Protection* 87, 44-49. DOI: 10.1016/j.cropro.2016.04.016

Guo, J., and Lua, A. C. (1999). "Textural and chemical characterisations of activated carbon prepared from oil-palm stone with H_2SO_4 and KOH impregnation," *Microporous and Mesoporous Materials* 32(1-2), 111-117. DOI: 10.1016/S1387-1811(99)00096-7

Gurten, I. I., Ozmak, M., Yagmur, E., and Aktas, Z. (2012). "Preparation and characterisation of activated carbon from waste tea using K_2CO_3," *Biomass & Bioenergy* 37(1), 73-78. DOI:10.1016/j.biombioe.2011.12.030

Hassan, A. F., Youssef, A. M., and Priecel, P. (2013). "Removal of deltamethrin insecticide over highly porous activated carbon prepared from pistachio nutshells," *Carbon Letters* 14(4), 234-242. DOI: 10.5714/CL.2013.14.4.234

Hayashi, J., Kazehaya, A., Muroyama, K., and Paul Watkinson, A. (2000). "Preparation of activated carbon from lignin by chemical activation," *Carbon* 38(13), 1873-1878. DOI: 10.1016/S0008-6223(00)00027-0

ISO 562 (1974). "Hard coal and coke; Determination of volatile matter content," International Organization for Standardization, Geneva, Switzerland.

ISO 589 (2008). "Hard coal - Determination of total moisture," International Organization for Standardization, Geneva, Switzerland.

ISO 1171 (1976). "Solid mineral fuels; Determination of ash," International Organization for Standardization, Geneva, Switzerland.

Kucherenko, V. A., Shendrik, T. G., Tamarkina, Y. V., and Mysyk, R. D. (2010). "Nanoporosity development in the thermal-shock KOH activation of brown coal," *Carbon* 48(15), 4556-4558. DOI: 10.1016/j.carbon.2010.07.027

Li, X. F., Luo, X. G., Dou, L. Q. and Chen, K. (2016). "Preparation and characterization of K_2CO_3-activated kraft lignin carbon," *BioResources* 11(1), 2096-2108. DOI: 10.15376/biores.11.1.2096-2108

Lu, J., Zhao, L., Ma, R., Zhang, P., Fan, R., and Zhang, J. (2010). "Performance of the biological control agent flea beetle *Agasicles hygrophila* (Coleoptera: Chrysomelidae), on two plant species *Alternanthera philoxeroides* (alligator weed) and *A. sessilis* (joyweed)," *Biological Control* 54(1), 9-13. DOI: 10.1016/j.biocontrol.2010.02.012

McFadyen, R. E. C. (1998). "Biological control of weeds," *Annual Review of Entomology* 43(1), 369-393. DOI: 10.1146/annurev.ento.43.1.369

Schooler, S. S., Yeates, A. G., Wilson, J. R. U., and Julien, M. H. (2007). "Herbivory, mowing, and herbicides differently affect production and nutrient allocation of *Alternanthera philoxeroides*," *Aquatic Botany* 86(1), 62-68. DOI: 10.1016/j.aquabot.2006.09.004

Schooler, S., Cook, T., Bourne, A., Prichard, G., and Julien, M. (2008). "Selective herbicides reduce alligator weed (*Alternanthera Philoxeroides*) biomass by enhancing competition," *Weed Science* 56(2), 259-264. DOI: 10.1614/WS-07-132.1

Sun, Y., Ding, J., and Frye, M. J. (2010). "Effects of resource availability on tolerance of herbivory in the invasive *Alternanthera philoxeroides* and the native *Alternanthera sessilis*," *Weed Research* 50(6), 527-536. DOI: 10.1111/j.1365-3180.2010.00822.x

Wei, D., Liping, C. P., Zhijun, M. J., Guangwei, W. W., and Ruirui, Z. R. (2010). "Review of non-chemical weed management for green agriculture," *International Journal of Agricultural and Biological Engineering* 3(4), 52-60. DOI:

10.3965/j.issn.1934-6344.2010.04.052-060

Wei, H., Lu, X., and Ding, J. (2015). "Direct and indirect impacts of different water regimes on the invasive plant, alligator weed (*Alternanthera philoxeroides*), and its biological control agent, *Agasicles hygrophila*," *Weed Biology Management* 15(1), 1-10. DOI: 10.1111/wbm.12055

Willingham, S. D., Bagavathiannan, M. V., Carson, K. S., Cogdill, T. J., McCauley, G. N., and Chandler, J. M. (2015). "Evaluation of herbicide options for alligatorweed (*Alternanthera philoxeroides*) control in rice," *Weed Technology* 29(4), 793-799. DOI: 10.1614/WT-D-14-00164.1

Yang, Y., Wei, Z., Zhang, X., Chen, X., Yue, D., Yin, Q., Xiao, L., and Yang, L. (2014). "Biochar from *Alternanthera philoxeroides* could remove Pb(II) efficiently," *Bioresource Technology* 171, 227-232. DOI: 10.1016/j.biortech.2014.08.015

Yan, L., and Sorial, G. A. (2011). "Chemical activation of bituminous coal for hampering oligomerization of organic contaminants," *Journal of Hazardous Materials* 197(24), 311-319. DOI: 10.1016/j.jhazmat.2011.09.093

Article submitted: November 24, 2016; Peer review completed: January 12, 2017; Revised version received: March 7, 2017; Accepted: March 8, 2017; Published: March 20, 2017.
DOI: 10.15376/biores.12.2.3340-3350